Effects of blood ΔR(2)* non-linearity on absolute perfusion quantification using DSC-MRI: Comparison with Xe-133 SPECT.

Knutsson, Linda; Ståhlberg, Freddy; Wirestam, Ronnie; van Osch, Matthias J

Published in:
Magnetic Resonance Imaging

DOI:
10.1016/j.mri.2012.12.001

2013

Effects of blood ΔR_2^* non-linearity on absolute perfusion quantification using DSC-MRI: Comparison with Xe-133 SPECT

Linda Knutsson, PhD,[1] Freddy Ståhlberg, PhD,[1,2] Ronnie Wirestam PhD,[1] Matthias J. van Osch, PhD,[3]

(1) Department of Medical Radiation Physics, Lund University, Lund, Sweden
(2) Department of Diagnostic Radiology, Lund University, Lund, Sweden
(3) Department of Radiology, Leiden University Medical Center, Leiden, The Netherlands

Correspondence to:
Assoc. Prof. Linda Knutsson

Department of Medical Radiation Physics

Lund University

Lund University Hospital

SE-221 85 Lund, Sweden

E-mail: Linda.Knutsson@med.lu.se

Fax: +46 46 178540

Short title: ΔR_2^* non-linearity in DSC-MRI perfusion quantification

Abstract

Purpose:

To evaluate whether a non-linear blood ΔR_2*-versus-concentration relationship improves quantitative cerebral blood flow (CBF) estimates obtained by dynamic susceptibility contrast (DSC) MRI in a comparison with Xe-133 SPECT CBF in healthy volunteers.

Material and Methods:

Linear as well as non-linear relationships between ΔR_2* and contrast agent concentration in blood were applied to the arterial input function (AIF) and the venous output function (VOF) from DSC-MRI. To reduce partial volume effects in the AIF, the arterial time integral was rescaled using a corrected VOF scheme.

Results:

Under the assumption of proportionality between the two modalities, the relationship CBF(MRI)=0.58CBF(SPECT) (r=0.64) was observed using the linear relationship and CBF(MRI)=0.51CBF(SPECT) (r=0.71) using the non-linear relationship.

Discussion:

A smaller ratio of the VOF time integral to the AIF time integral and a somewhat better correlation between global DSC-MRI and Xe-133 SPECT CBF estimates were observed using the non-linear relationship. The results did not, however, confirm the superiority of one model over the other, potentially because realistic AIF signal data may well originate from a combination of blood and surrounding tissue.

Key words: perfusion; dynamic susceptibility contrast MRI; blood relaxivity; SPECT

Introduction

Reproducible absolute quantification of cerebral blood flow (CBF) using dynamic susceptibility contrast MRI (DSC-MRI) is difficult since several steps in the data acquisition and processing are associated with inaccuracies. For example, partial volume effects (PVEs) [1], arterial signal saturation at peak concentration [2], local geometric distortion (leading to arterial signal relocation) during the bolus passage [3] and the concentration-dependent difference in T2* relaxivity between tissue and large vessels [4,5] are all factors that influence the absolute quantification of CBF.

In an attempt to minimise the influence of PVEs on the arterial input function (AIF) time integral, Knutsson et al. [6] rescaled the AIF using a corrected venous output function (VOF). Using this approach the correlation between CBF estimates obtained by DSC-MRI and Xe-133 single photon emission computed tomography (SPECT) was improved. However, in that evaluation a linear relationship between the ΔR_2^* and contrast agent concentration in blood was assumed, while gradient-echo based calibration measurements in whole blood have shown that a non-linear relation between ΔR_2^* and contrast agent concentration exists [7].

In realistic AIF measurements, however, the AIF signal may well originate from a combination of blood and surrounding tissue, in unknown proportions (which, additionally, may vary during the bolus passage). Considering that the tissue ΔR_2^* response to the contrast agent is linear [4], and that extravascular spins in the vicinity of large vessels show a non-trivial ΔR_2^*-versus-concentration relationship (which under certain specific conditions can be linear) [8], it is difficult to predict whether it would be most appropriate to apply a linear or a non-linear ΔR_2^*-versus-concentration relationship to a practical AIF measurement.

In this re-evaluation of CBF data, we thus empirically compared quantitative CBF estimates obtained by DSC-MRI and Xe-133 SPECT [6], using both a linear and a non-linear relationship for blood when applying the VOF correction scheme to DSC-MRI data from healthy subjects.

Material and Methods

Whole-brain CBF was measured using Xe-133 SPECT and DSC-MRI in 20 healthy volunteers. The subjects were 7 men and 13 women, 43 – 81 years old (average age 66 years) at the time of the Xe-133 SPECT examination. The Xe-133 SPECT measurement was performed before the DSC-MRI experiment. The time interval between the Xe-133 SPECT experiment and the DSC-MRI measurement was on average 19 months (range 9-25 months). Prior to the CBF measurements, each individual was examined by specialists in psychiatry and dementia. The project was approved by the local ethics committee and informed consent was obtained from all volunteers.

Xe-133 SPECT

A three-head scintillation camera (Picker Prism 3000XP) was used for the Xe-133 SPECT acquisition. Xe-133 gas (500 MBq/l in air) was inhaled during 8 minutes followed by 22 minutes of breathing of ordinary air. Ten slices were reconstructed with a nominal slice thickness of 7.1 mm and the image matrix was 64×64. CBF was calculated using a bi-exponential analysis developed by Obrist et al. [9] and modified by Risberg et al. [10]. Cerebral blood flow was calculated by using a slope index (SI) when evaluating whole-brain CBF and grey matter CBF, and this index was calculated in a similar way as the initial slope index of the two-dimensional Xe-133 inhalation method [10]. The white matter was evaluated using a parameter accounting for fast as well as the slow flow component, $w \cdot SI+(1-w) \cdot FWM$, where w is the relative weight factor of the fast component (represented by SI) in each pixel and FWM is the slow flow component of WM.

DSC-MRI

The DSC-MRI examinations were performed using a 3T head scanner (Magnetom Allegra, Siemens AG, Erlangen, Germany). All volunteers received a gadolinium contrast-agent dose of 0.1 mmol per kg bodyweight (Magnevist®, Schering AG, Berlin, Germany) injected automatically at a rate of 5 ml/s in an arm vein followed by a saline flush. The contrast-agent bolus was monitored in 23 slices by use of a gradient-echo echo-planar imaging (GRE-EPI) pulse sequence with flip angle 90^{o}, echo time 21 ms, slice thickness 5 mm and image matrix 128×128. Sixty images per slice were recorded in the time series with a temporal resolution of 1.5 s.

CBF was calculated using Zierler's area-to-height relationship and the central volume principle [11,12]:

$$CBF = \frac{(1-H_{\text{large}})\, R_{\max} \int_0^{\infty} C(t)dt}{\rho(1-H_{\text{small}}) \int_0^{\infty} R(t)dt \int_0^{\infty} C_{art}(t)dt} \qquad (1)$$

where C is the contrast-agent concentration in tissue and C_{art} is the contrast-agent concentration in a brain-feeding artery. By deconvolving the measured tissue concentration time curve C(t) with an AIF, the tissue residue function R(t) can be obtained and R_{max} is the peak value of this function. H_{large} and H_{small} are the haematocrit values in large and small vessels, respectively, and ρ is the whole-brain mass density. The value $(1\text{-}H_{large})/[\rho\ (1\text{-}H_{small})]$ = 0.705 cm^3/g was used in this study [13]. Deconvolution was accomplished using a block-circulant singular value decomposition algorithm [14] with a fixed cutoff of 10%, and a global arterial input function was obtained from middle cerebral artery branches in the Sylvian

fissure region. The arterial and venous concentration time curves were calculated using a linear relationship (Eq. 2) as well as a non-linear relationship (Eq. 3) between the transverse relaxation-rate change $\Delta R^*_2(t)$ and contrast-agent concentration in blood (C_{blood}) [15]:

$$\Delta R^*_2(t) = r_{2GdDTPA} C_{blood}(t) \quad (2)$$

where $r_{2GdDTPA}$ is the transverse relaxivity, assumed to be 20 $mM^{-1}s^{-1}$. This relaxivity is an approximation based on a linear fit to ΔR^*_2-versus-C data obtained from the relationship in Eq. 3 below, using concentration values in the range 0 – 10 mM.

$$\Delta R^*_2(t) = a_1 C_{blood}(t) + a_2 C_{blood}(t)^2 \quad (3)$$

where a_1 was set to 0.49 $mM^{-1}s^{-1}$and a_2 to 2.6 $mM^{-2}s^{-1}$ [16].

Since negative concentration-time-values cannot be obtained from the non-linear model, the concentration-time-values for negative $\Delta R^*_2(t)$, using the non-linear approach, were calculated using a linear approximation of Eq. 3 adapted to very low concentration levels (0-1.4). For improved absolute quantification of the DSC-MRI-based CBF estimates, a rescaling of the arterial concentration time integral was introduced (based on the assumption that true arterial and venous time integrals are to be identical) using an approximate VOF [6]. Using this rescaling signal time curves in the superior sagittal sinus as well as in a small vein at a section superior to the confluence sinuum were selected manually. The concentration time curve from the small vein was then time shifted (if necessary) and multiplied by an amplification factor in order to match the base and flanks of the superior sagittal sinus concentration–time curve leading to an approximate VOF. This rescaling procedure was applied to blood concentration time curves calculated using the linear relationship as well as

the non-linear relationship. The tissue curves C(t) were, in both cases, calculated according to $\Delta R^*_2(t) = r_{2GdDTPA} C(t)$ using the transverse relaxivity value of 87 $mM^{-1}s^{-1}$ [16].

Evaluation

Only signal-versus-time curves exceeding a certain baseline signal threshold were included in the perfusion analysis. DSC-MRI CBF values exceeding 2.5 times the mean CBF from all voxels were assumed to originate from large vessels and thus excluded from the data analysis. To match the slices from the Xe-133 SPECT measurement the 23 CBF slices from the MRI data were reconstructed into 10 slices. Whole-brain average CBF estimates, calculated from a comprehensive selection of regions of interest (ROIs) excluding non-tissue voxels, obtained by the DSC-MRI technique and the Xe-133 SPECT method were compared. In addition, bilateral ROIs in thalamus grey matter (GM), and frontal white matter (WM) were evaluated separately with respect to CBF.

Bland-Altman analysis were performed on the CBF data in order to enable a statistical interpretation of the results. Furthermore, the coefficients of correlation obtained using the two approaches were statistically analysed.

Results

DSC-MRI showed an average whole-brain CBF of 23 ± 9 ml/(min 100 g) using the linear relationship between ΔR_2* and concentration and 20 ± 8 ml/(min 100 g) using the non-linear relationship. The Xe-133-SPECT measurements resulted in a corresponding average whole-brain CBF of 40 ± 8 ml/(min 100 g).

Figure 1 shows the individual data points, displayed as CBF(MRI) versus CBF(SPECT) using the two models. The relationship between the CBF estimates obtained by the two modalities was CBF(MRI)=0.81CBF(SPECT)-9.2, with a correlation coefficient of r=0.67 (p=0.0012, 95% confidence interval 0.33 to 0.86), using the linear ΔR_2*-versus-concentration relationship. For the non-linear ΔR_2*-versus-concentration relationship, the corresponding CBF relationship between the two modalities was CBF(MRI)=0.80CBF(SPECT)-12, with a correlation coefficient of r=0.76 (p=0.0001, 95% confidence interval 0.48 to 0.90). The correlation coefficients observed with the linear and non-linear approaches were not significantly different (Fisher r-to-z transformation, p=0.59). Under the assumption of proportionality between the two modalities, the relationship CBF(MRI)=0.58CBF(SPECT) (r=0.64) was observed using the linear relationship and CBF(MRI)=0.51CBF(SPECT) (r=0.71) using the non-linear relationship.

In GM regions, the average Xe-133 SPECT based CBF was 44 ± 10 ml/(min 100 g) while the corresponding DSC-MRI-based CBF estimate was 32 ± 14 ml/(min 100 g) using the linear relationship and 28 ± 12 ml/(min 100 g) using the non-linear relationship. In frontal WM the DSC-MRI experiment resulted in a CBF estimate of 14 ± 5 ml/(min 100 g) using the linear

relationship and 12 ± 5 ml/(min 100 g) using the non-linear relationship, while Xe-133 SPECT showed 22 ± 4 ml/(min 100 g)

The MRI-versus-SPECT CBF relationship in GM and WM is displayed in Fig. 2. The relationship between the CBF estimates in GM and WM obtained by the two modalities was CBF(MRI)=0.96CBF(SPECT)-7.7 (r=0.86) using the linear relationship and CBF(MRI)=0.85CBF(SPECT)-7.1 (r=0.86) using the non-linear relationship. Under the assumption of proportionality between the two modalities, the relationship CBF(MRI)=0.75CBF(SPECT) (r=0.84) was observed using the linear relationship and CBF(MRI)=0.66CBF(SPECT) (r=0.84) using the non-linear relationship.

The average ratio of the VOF time integral to the AIF time integral was 1.8 ± 0.62 using the linear relationship and 1.3 ± 0.45 using the non-linear relationship. Figure 3 displays an example of the shape of the concentration time curve using the linear and non-linear approaches, calculated from a typical signal time curve retrieved from the superior sagittal sinus. The base and flanks were typically steeper using the linear approach leading to a higher average ratio between the time integral of the corrected VOF and the time integral of the measured AIF.

Bland-Altman plots for the whole-brain CBF estimates obtained by the two modalities are shown in Figure 4.

Discussion

In this study, the effects of applying a non-linear instead of a linear relationship between ΔR_2^* and contrast agent concentration in blood were examined on experimental DSC-MRI data by comparing the calculated CBF estimates to Xe-133 SPECT CBF data. Applying a non-linear relationship slightly improved the correlation between DSC-MRI data and SPECT with regard to whole-brain CBF, although no significant improvement could be detected.

In the present study, the bolus passage was registered in three different vessels; the assumed correct shapes of the AIF and VOF were measured in a small artery and a small vein, respectively, and the VOF was subsequently fitted to the measured concentration curve of the sagittal sinus, which was assumed to be saturated but uncorrupted by PVEs. The non-linear relationship was applied to all three measurements, resulting in a similar observed degree of correlation with the SPECT data as when a linear relationship was applied to the AIFs and VOFs. This was further concluded when the statistical test comparing the two correlation coefficients showed that the methods were not significantly different. It is thus difficult to draw any firm conclusions about the importance of applying the non-linear model from such a small difference in the correlation coefficients between the two models, considering other uncertainties present in the measurement and evaluation procedure.

The choice of venous output functions in the superior sagittal sinus and in the small vein [6] requires a user interaction that can be challenging in some cases, and this constitutes a potential source of inaccuracy. Even if the sagittal sinus is a large vein, the selected voxel probably does not contain 100% blood due to the limited spatial resolution of the DSC-MRI experiment. Furthermore, the shapes of the contrast passage curves could very well have been

affected by non-linear PVEs [7], whereas the current PVE approach will only correct for errors in the curve areas. Further errors in the method could be an incorrect shape of the small-vein curve and/or of the flanks of the distorted sagittal-sinus curve, leading to an error in the VOF time integral. However, the reproducibility of this PVE correction scheme has been examined and shown to be quite satisfactory (correlation between repeated analyses was r=0.87) [17]. The non-linear approach was applied to the AIF and the small vein, but since these smaller vessels suffered from PVEs it is obvious that the signal in these cases did not originate from blood only. Furthermore, the non-linearity between ΔR_2^* and contrast agent concentration observed in ref [7] was obtained from fully oxygenated blood and not venous blood. The T2* is different in venous blood and this could influence the non-linear relationship.

Application of both the linear and the non-linear relationship led, in general, to an underestimation of CBF as compared to SPECT. The absolute CBF values depend, however, strongly on the T2* relaxivity set by the user. The value used for tissue in this study, i.e., 87 $mM^{-1}s^{-1}$, was taken from the theoretical model of Kjølby et al. [16], but this value could very well be too high, since the study from Kjølby et al. assumed that the magnetic field disturbance of each vessel does not interact with magnetic field disturbances of neighbouring vessels. This assumption probably does not hold true for the maximum concentration of contrast agent in the grey matter, as apparent from the large signal drop (>50%) predicted by data from Kjølby et al. If using a lower tissue relaxivity value, the CBF estimates would be increased and closer to what is typically obtained by gold-standard methods. Furthermore, the value used for blood in this study, i.e. 20 $mM^{-1}s^{-1}$, is taken from a linear approximation based on data from the non-linear model, and this approximation is highly dependent on the range of concentrations included in the linear fit. For example, using a concentration range of 0 – 15

mM would result in a T2* relaxivity of 30 $mM^{-1}s^{-1}$ and correspondingly higher absolute CBF values from the linear model. It should be noted that the selected linear tissue relaxivity, set by the user, does not influence the degree of correlation between DSC-MRI and SPECT for the two methods, since it only acts as a scaling factor of the quantitative CBF values.

The average ratio of the corrected VOF time integral to the AIF time integral was 38% lower using the non-linear relationship. This is probably due to the fact that the distorted peaks become less pronounced at high concentration when applying the non-linear correction, as demonstrated in Figure 3.

Previously, the two approaches have been examined using simulations. Calamante et al. [15] simulated DSC-MRI data for a range of tissue types using both the linear and non-linear relationship for the AIF. Both absolute and relative CBF values were investigated and it was shown that the non-linear relationship led to more accurate absolute CBF estimates than the linear assumption. This suggests that, in the analysis of DSC-MRI data, the non-linear relationship should be used when the AIF is measured within the artery.

In a study by Zaharchuk et al. [18], a correction for both non-linearity and PVEs was applied to DSC-MRI data. The DSC-MRI CBF estimates were then compared to CBF values retrieved using stable xenon computed tomography, and no difference in the mean correlation coefficients obtained with and without non-linearity correction was observed. Contrary to our study, no correction scheme for geometric distortions and signal saturation was applied to the VOF time integral which might have led to a larger remaining PVE effect in the rescaled AIF time integral.

Conclusion

Experimental data showed no significant difference in the correlation between Xe-133 SPECT CBF and AIF-rescaled DSC-MRI CBF when applying the two different ΔR2*-versus-concentration relationships to AIF and VOF data. However, a slight improvement in correlation for whole-brain CBF as well as a smaller ratio of the corrected VOF time integral to the measured AIF time integral was observed when applying the non-linear approach.

Acknowledgments

This study was supported by the Swedish Research Council (grant nos. 13514, 2005-6910, 2007-3974 and 2007-6079), the Crafoord foundation, the Lund University Hospital Donation Funds and the Swedish Cancer Society, grant no. 2009/1076.

References

1. van Osch, MJ, van der Grond J, Bakker CJ. Partial volume effects on arterial input functions: shape and amplitude distortions and their correction. J Magn Reson Imaging, 2005;22:704-709.
2. Ellinger R, Kremser C, Schocke MF et al. The impact of peak saturation of the arterial input function on quantitative evaluation of dynamic susceptibility contrast-enhanced MR studies. J Comput Assist Tomogr 2000;24:942 -948.
3. Rausch M, Scheffler K, Rudin M, Radu EW. Analysis of input functions from different arterial branches with gamma variate functions and cluster analysis for quantitative blood volume measurements. Magn Reson Imaging 2000;18:1235-1243.
4. Kjølby BF, Østergaard L, Kiselev VG. Theoretical model of intravascular paramagnetic tracers effect on tissue relaxation. Magn Reson Med 2006;56:187–197.
5. Kiselev VG. On the theoretical basis of perfusion measurements by dynamic susceptibility contrast MRI. Magn Reson Med 2001;46:1113–1122.
6. Knutsson L, Börjesson S, Larsson EM, et al. Absolute quantification of cerebral blood flow in normal volunteers: Correlation between Xe-133-SPECT and dynamic susceptibility contrast MRI. J Magn Reson Imaging 2007;26:913-920.
7. van Osch MJP, Vonken EPA, Viergever MA, van der Grond J, Bakker CJG. Measuring the arterial input function with gradient echo sequences. Magn Reson Med 2003;49:1067-1076.
8. Bleeker EJ, van Buchem MA, van Osch MJ. Optimal location for arterial input function measurements near the middle cerebral artery in first-pass perfusion MRI. J Cereb Blood Flow Metab 2009;29:840-852.
9. Obrist WD, Thompson HK, Wang HS, Wilkinson WE. Regional cerebral blood flow estimated by 133-xenon inhalation. Stroke 1975;6:245-256.

10. Risberg J, Ali Z, Wilson EM, Wills EL, Halsey JH. Regional cerebral blood flow by 133-xenon inhalation. Stroke 1975;6:142-148.
11. Zierler KL. Equations for measuring blood flow by external monitoring of radioisotopes. Circ Res. 1965;16:309-321.
12. Meier P, Zierler KL. On the theory of indicator-dilution method for measurement of blood flow and volume. J Appl Physiol 1954;6:731-744.
13. Rempp KA, Brix G, Wenz F, Becker CR, Gückel F, Lorenz WJ. Quantification of regional cerebral blood flow and volume with dynamic susceptibility contrast-enhanced MR imaging. Radiology 1994;193:637-641.
14. Wu O, Østergaard L, Weisskoff RM, Benner T, Rosen BR, Sorensen AG. Tracer arrival timing-insensitive technique for estimating flow in MR perfusion-weighted imaging using singular value decomposition with a block-circulant deconvolution matrix. Magn Reson Med. 2003;50:164-174.
15. Calamante F, Connelly A, van Osch MJ. Nonlinear DeltaR*2 effects in perfusion quantification using bolus-tracking MRI. Magn Reson Med 2009;61:486-49.
16. Kjølby BF, Mikkelsen IK, Pedersen M, Østergaard L, Kiselev VG. Analysis of partial volume effects on arterial input functions using gradient echo: a simulation study. Magn Reson Med. 2009;61:1300-1309.
17. Knutsson L, Wirestam R, Petersen ET, Markenroth Bloch K, Ståhlberg F, Holtås S, van Westen D. Absolute quantification of cerebral blood flow using dynamic susceptibility contrast MRI: a comparison with model-free arterial spin labelling. Oral presentation at the 25th Annual Meeting of the European Society for Magnetic Resonance in Medicine and Biology. October 2-4, 2008, Valencia, Spain
18. Zaharchuk G, Bammer R, Straka M, et al. Improving dynamic susceptibility contrast MRI measurement of quantitative cerebral blood flow using corrections for partial

volume and nonlinear contrast relaxivity: A xenon computed tomographic comparative study. J Magn Reson Imaging. 2009;30:743-52.

Figure legend

Figure 1.

Whole-brain cerebral blood flow estimates, nominally in ml/(min 100 g), obtained using Xe-133 SPECT and DSC-MRI in 20 healthy volunteers using the linear relationship (top) and the non-linear relationship (bottom) between ΔR_2*and contrast-agent concentration in blood.

Figure 2.

Grey matter (diamonds) and white matter (triangles) cerebral blood flow estimates, nominally in ml/(min 100 g), obtained using Xe-133 SPECT and DSC-MRI in 20 healthy volunteers using the linear relationship (top) and the non-linear relationship (bottom) between ΔR_2*and contrast-agent concentration in blood.

Figure 3.

(a) Signal-time curve obtained from the sagittal sinus and the corresponding concentration time curve calculated using (b) the linear approach and (c) the non-linear approach.

Figure 4.

Bland-Altman plots for the whole-brain cerebral blood flow estimates obtained by DSC-MRI and Xe-133 SPECT, using the linear relationship (top) and the non-linear relationship (bottom) between ΔR_2*and contrast agent concentration for arterial and venous DSC-MRI data. Red lines are 1.96×S.D. and the green line is the mean difference between the two populations.

Figure 1

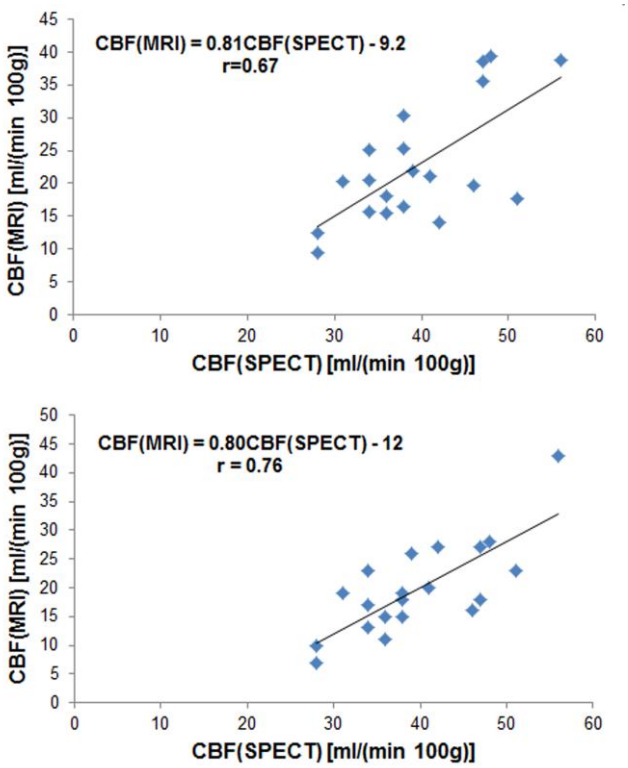
CBF(MRI) = 0.81CBF(SPECT) - 9.2
r=0.67
CBF(MRI) [ml/(min 100g)]
CBF(SPECT) [ml/(min 100g)]
CBF(MRI) = 0.80CBF(SPECT) - 12
r = 0.76
CBF(MRI) [ml/(min 100g)]
CBF(SPECT) [ml/(min 100g)]

Figure 2

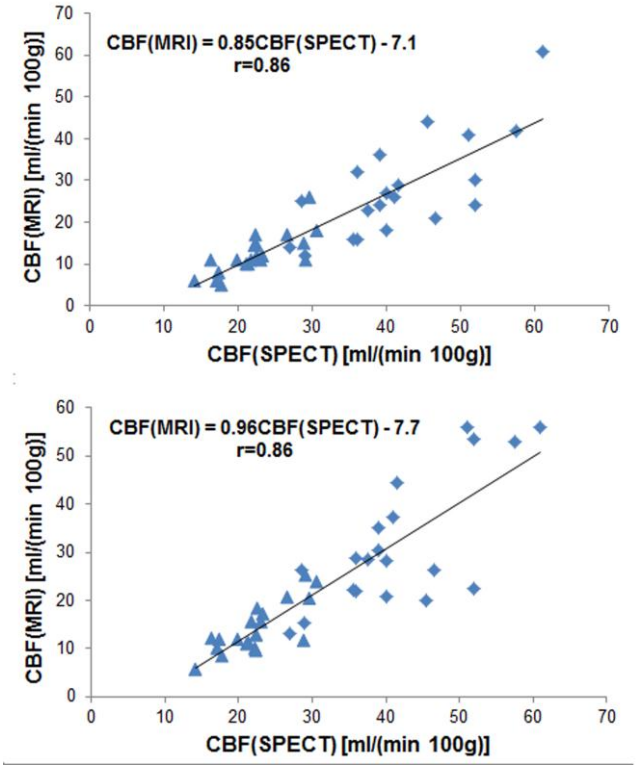
CBF(MRI) = 0.85CBF(SPECT) - 7.1
r=0.86
CBF(MRI) [ml/(min 100g)]
CBF(SPECT) [ml/(min 100g)]
CBF(MRI) = 0.96CBF(SPECT) - 7.7
r=0.86
CBF(MRI) [ml/(min 100g)]
CBF(SPECT) [ml/(min 100g)]

Figure 3

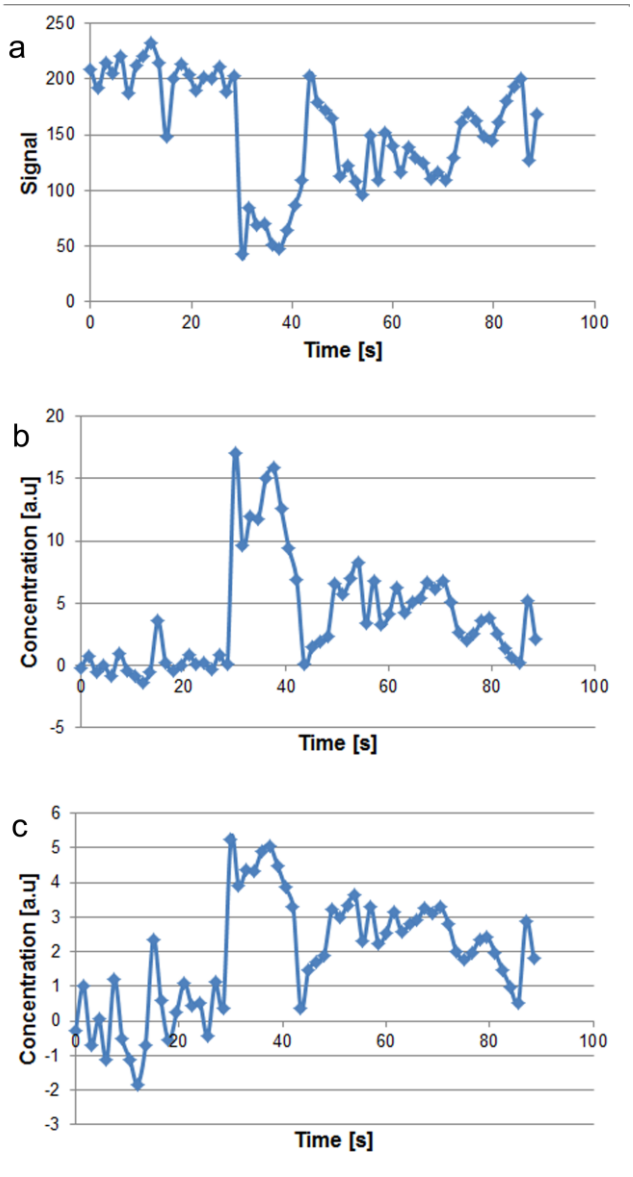
a
Signal
250
200
150
100
50
0
0
20
40
60
80
100
Time [s]
b
Concentration [a.u]
20
15
10
5
0
-5
0
20
40
60
80
100
Time [s]
c
Concentration [a.u]
6
5
4
3
2
1
0
-1
-2
-3
0
20
40
60
80
100
Time [s]

Figure 4

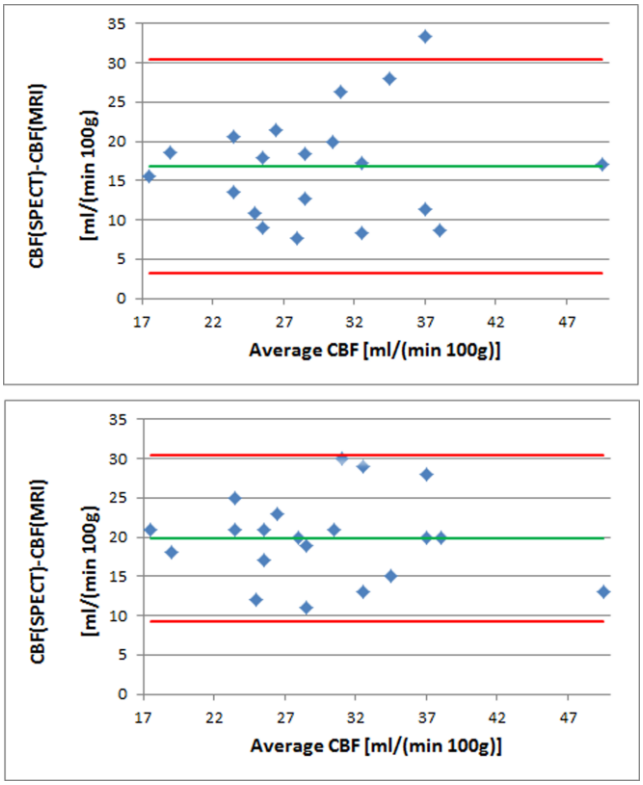
CBF(SPECT)-CBF(MRI) [ml/(min 100g)]
35
30
25
20
15
10
5
0
17
22
27
32
37
42
47
Average CBF [ml/(min 100g)]
CBF(SPECT)-CBF(MRI) [ml/(min 100g)]
35
30
25
20
15
10
5
0
17
22
27
32
37
42
47
Average CBF [ml/(min 100g)]